

963

964

965

966

967

968 **Supporting Information for**

969 2-Thiouridine is a broad-spectrum antiviral nucleoside analogue
970 against positive-strand RNA viruses.

971

972 Kentaro Uemura, Haruaki Nobori, Akihiko Sato, Shinsuke Toba, Shinji Kusakabe, Michihito

973 Sasaki, Koshiro Tabata, Keita Matsuno, Naoyoshi Maeda, Shiori Ito, Mayu Tanaka, Yuki

974 Anraku, Shunsuke Kita, Mayumi Ishii, Kayoko Kanamitsu, Yasuko Orba, Yoshiharu Matsuura,

975 William W. Hall, Hirofumi Sawa, Hiroshi Kida, Akira Matsuda, and Katsumi Maenaka

976

977 Katsumi Maenaka

978 Email: maenaka@pharm.hokudai.ac.jp

979

980 **This PDF file includes:**

981

982 Supporting text

983 Figures S1 to S11

984 Tables S1 to S5

985 SI References

986

987

988 **Supporting text**

989

990 **Materials & Methods**

991 *In vitro* growth kinetics of drug-resistant mutants

992 VeroE6 cells were seeded onto 24-well plates the previous day and were
993 infected with rgDENV2 (rgDENV2-WT or rgDENV2-NS5-G605V) at an MOI of
994 0.01 for 1 h. After incubation, the unbound virus was removed, and new medium
995 was added. At 24, 48, 72, and 96 hpi, total RNA was isolated with PureLink RNA
996 Mini Kit. Viral RNA level was quantified by qRT-PCR analysis as described above
997 with *ACTB* transcripts used as internal controls.

998

999 Mitochondrial protein synthesis assays

1000 HepG2 cells were seeded onto 96-well plates the previous day and treated
1001 with the 3-fold serially diluted compound ($n = 2$). At 5 dpi, one set of plates was
1002 fixed with 4% paraformaldehyde (Nacalai tesque) and the intracellular levels of
1003 two mitochondrial proteins, the mitochondrial DNA-encoded cytochrome c
1004 oxidase I (COX-I) and nuclear DNA-encoded succinate dehydrogenase A (SDH-
1005 A) were determined using the MitoBiogenesis In-Cell Enzyme-linked
1006 immunosorbent assay (ELISA) Kit (Colorimetric, Abcam, ab110217) following the
1007 manufacturer's instructions. To monitor the cell viability as an ATP level, the
1008 second set of plates was analyzed by adding CellTiter-Glo 2.0 Reagent (Promega,
1009 G9242/3) and measuring luminescence on a GloMax Discover System
1010 (Promega). The IC_{50} value was defined in GraphPad Prism version 8.4.3 with a
1011 variable slope (four parameters).

1012

1013 Establishment of mouse-adapted DENV2 and SARS-CoV-2

1014 AG129 mice (IFN- α/β and IFN- γ receptors deficient 129/Sv mice) were
1015 purchased from Marshall BioResources and bred in-house under the specific
1016 pathogen-free (SPF) conditions. To establish mouse-adapted DENV2, named
1017 DENV2 AG-P10 strain, virus passage in mice was carried out according to a
1018 previous report (1). Briefly, 7-weeks-old female AG129 mice were inoculated
1019 intraperitoneally with 100 μ L of 4×10^5 PFU/mouse of DENV2 D2/hu/INDIA/09-74
1020 strain. On day 3 after infection, the infected mice were euthanized under deep
1021 anesthesia by isoflurane inhalation, and serum was collected. Virus in the serum
1022 was amplified in C6/36 cells and then intraperitoneally injected into other AG129
1023 mice. This adaptation process was performed a total of 10 times.

1024 To establish mouse-adapted SARS-CoV-2, named SARS-CoV-2 MA-P10
1025 strain, virus passage in mouse was carried out according to a previous report (2,
1026 3). Briefly, SPF, 30–45-week-old female BALB/c mice (BALB/cAJcl, CLEA Japan)
1027 were inoculated intranasally with 50 μ L of 1×10^5 TCID₅₀/mouse of SARS-CoV-2
1028 WK-521 strain under anesthesia. On day 3 after infection, the infected mice were

1029 euthanized, and whole lung tissues were harvested and homogenized in DMEM
1030 supplemented with 10% FBS and P/S with TissueRuptor (Qiagen). Virus in the
1031 supernatants of lung homogenates were intranasally injected into other BALB/c
1032 mice. This adaptation process was performed a total of 10 times.

1033 Viral RNA was extracted and purified using QIAamp Viral RNA Mini Kit
1034 (Qiagen) according to the manufacturer's instructions. Next-generation
1035 sequencing (NGS) was conducted on an iSeq 100 System (Illumina, Inc.) and the
1036 sequences were analyzed using CLC Genomics Workbench ver. 21.0.3 software
1037 (CLC bio, Qiagen).

1038

1039 *In vitro* ADME assay

1040 Solubility assay: The Japanese Pharmacopeia (JP) 1st fluid (pH 1.2) or JP 2nd
1041 fluid (pH 6.8) for dissolution testing was used for solubility measurements. A test
1042 solution of test compound was prepared by diluting 10 mM DMSO stock solution
1043 2 μ L:165 μ L in JP1st or 2nd fluid and mixed at 37°C for 4 h by rotation at 1,000
1044 rpm. After loading the mixed solution into 96-well MultiScreen Filter Plates
1045 (product number MSHVN4510, 0.45 μ m hydrophilic PVDF membrane, Millipore),
1046 filtration was performed by centrifugation. The filtrates were mixed with
1047 acetonitrile and analyzed by HPLC-UV (254 nm). Solubility was calculated by
1048 comparing the peak area of the filtrate mixture with that of a 100 μ M standard
1049 solution. When the peak area of the filtrate mixture was larger than the peak area
1050 of the standard solution, it was described as >100 μ M.

1051 PAMPA assay to determine the passive membrane diffusion rates: A Corning
1052 Gentest Pre-coated PAMPA Plate System was used in the PAMPA permeability
1053 test. The acceptor plate was prepared by adding 200 μ L of 5% DMSO/0.1 M
1054 phosphate buffer (pH 7.4) to each well, and then 300 μ L of 100 μ M test
1055 compounds in 5% DMSO/0.1 M phosphate buffer (pH 6.4) was added to the
1056 donor wells. The acceptor plate was then placed on top of the donor plate and
1057 incubated at 37°C without agitation for 4 h. At the end of the incubation, the plates
1058 were separated and the solutions from each well of both the acceptor plate and
1059 the donor plate were transferred to 96-well plates and mixed with acetonitrile and
1060 water. The final concentrations of compounds in both the donor wells and
1061 acceptor wells, as well as the concentrations of the initial donor solutions, were
1062 analyzed by liquid chromatography tandem mass spectrometry (LC-MS/MS). The
1063 permeability of the compounds was calculated according to a previous report (4).
1064 The recovery of tested compounds was more than 90%. The permeabilities of
1065 Antipyrine (100 μ M), Metoprolol (500 μ M) and Sulfasarazine (500 μ M) as
1066 reference compounds, with 100%, 95%, and 13% gastrointestinal absorptions in
1067 humans (4), were 11, 1.5 and 0.055×10^{-6} cm/s, respectively.

1068 Hepatic microsomal stability assay: Disappearance of the parent compound
1069 over time was measured by using the amount of drug at time zero as a reference.

1070 After 5 min of preincubation, 1 mM NADPH (final concentration, the same applies
1071 to the following) was added to a mixture containing 1 μ M of the test compound,
1072 0.2 mg/mL of human (pooled 200 individuals of mixed gender) or mouse (CD1
1073 male) liver microsomes (purchased from Sekisui XenoTech LLC), 1 mM EDTA
1074 and 0.1 M phosphate buffer (pH 7.4) and incubated at 37°C for 30 min by rotation
1075 at 60 rpm. An aliquot of 50 μ L of the incubation mixture was sampled and added
1076 to 250 μ L of chilled acetonitrile/internal standard (IS). After centrifuging for 15 min
1077 at $3,150 \times g$ (4°C), the supernatants were diluted with water and analyzed by LC-
1078 MS/MS. Hepatic microsomal stability (mL/min/kg, CL_{int}) was calculated according
1079 to a previous report (5), using 48.8 (human) or 45.4 (mouse) mg MS protein/g
1080 liver and 25.7 (human) or 87.5 (mouse) g liver/kg body weight as scaling factors.

1081 Determination of the unbound fraction in human or mouse plasma: An
1082 equilibrium dialysis apparatus was used to determine the unbound fraction for
1083 each compound in human or mouse plasma. High Throughput Dialysis Model
1084 HTD96b and Dialysis Membrane Strips MWCO 12-14 kDa obtained from
1085 HTDialysis, LLC (Gales Ferry, CT) were used. Plasma was spiked with the test
1086 compound (1 μ M), and 150 μ L aliquots were loaded into the apparatus and
1087 dialyzed versus 150 μ L of 0.1 M phosphate buffer (pH 7.4) at 37°C for 6 h by
1088 rotation at 80 rpm. The unbound fraction was calculated as the ratio of receiver
1089 side (buffer) to donor side (plasma) concentrations.

1090

1091 *In vivo* pharmacokinetics assay

1092 Five-week-old female BALB/c mice (purchased from Japan SLC) were treated
1093 with s2U by oral (150 mg/kg) or intravenous (20 mg/kg) administration. Blood was
1094 collected from the mouse tail with heparin 5 min, 15 min, 30 min, 1 h, 2 h, 4 h, 8
1095 h and 24 h after administration, and plasma samples were isolated at 2,000 rpm
1096 for 5 min.

1097 Plasma samples were precipitated with 4–8 volumes of acetonitrile/IS and
1098 centrifuged at $15,000 \times g$ at 4°C for 10 min. The supernatants were diluted with 7
1099 volumes of water and analyzed by LC-MS/MS. Standard non-compartmental
1100 analysis was performed to determine the pharmacokinetic parameters and to
1101 simulate the repeated dose concentration time profiles using Phoenix WinNonlin
1102 ver 8.3 (Pharsight): the estimated initial concentration (C_0), maximum plasma
1103 concentration (C_{max}), time to maximum plasma concentration (T_{max}), elimination
1104 half-life ($t_{1/2}$), area under the concentration time curve from time zero to infinity
1105 (AUC_{∞}), total clearance (CL_{tot}), and volume of distribution at terminal phase (V_{dz}).
1106 The absolute bioavailability (BA) of the oral dose was calculated as
1107 $AUC_{\infty}(po)/AUC_{\infty}(iv)$.

1108

1109 LC-MS/MS quantification method

1110 A Qtrap 6500+ mass spectrometer (Sciex) equipped with a Shimadzu Nexera
1111 series LC system (Shimadzu) was used. All compounds were analyzed in multi-
1112 reaction monitoring mode under electron spray ionization conditions. The
1113 analytical column used was an Acquity UPLC HSS T3 (1.8 μm , 3 \times 50 mm,
1114 Waters) at 40°C. The gradient mobile phase consisted of 0.1% formic acid in
1115 water (mobile phase A) and 0.1% formic acid in methanol (mobile phase B) at a
1116 total flow rate of 0.5 mL/min. The initial mobile phase composition was 2% B,
1117 which was held constant for 0.1 min, increased in a linear fashion to 90% B over
1118 0.9 min, then held constant for 1.5 min, and finally brought back to the initial
1119 condition of 2% B over 0.01 min and re-equilibrated for 2.5 min. The transitions
1120 (precursor ion > product ion) of s2U and IS (antipyrine) were 261.1 > 129.0 and
1121 189.0 > 56.0 (positive), respectively.

1122

1123 Bacterial reverse mutation test

1124 Each strain was tested using the direct method (in the absence of the S9
1125 metabolic activation system) and the metabolic activation method (in the
1126 presence of the S9 metabolic activation system). 0.1 mL of the s2U or control
1127 solution was added to 0.5 mL of 0.1 mol/L Na-phosphate buffer (pH 7.4) (direct
1128 method) or S9 mix (metabolic activation method). In addition, 0.1 mL of culture
1129 medium was added. The bacteria were then preincubated at 37°C for 20 min.
1130 After the pre-incubation, 2 mL of medium for stratification containing 0.05 mM L-
1131 histidine and 0.05 mM D-biotin (*Salmonella typhimurium*) or 0.05 mM L-
1132 tryptophan (*Escherichia coli*) were mixed in and were incubated at 37°C for 49
1133 hours. All plates of each strain were checked for growth inhibition using a
1134 stereomicroscope. The presence or absence of precipitation of the s2U was also
1135 checked visually. Next, the number of reversion mutant colonies was measured
1136 using a colony analyzer with area correction. These tests were performed by the
1137 Drug Safety Testing Center Co., Ltd. (Saitama).

1138

1139 *In vitro* gene mutation test using the Hprt genes in V79 cells

1140 Approximately 2×10^7 V79 cells in the logarithmic growth phase were mixed
1141 with s2U or positive control and tested with or without S9 metabolic activation
1142 system (direct method or metabolic activation method). Approximately 2×10^6
1143 cells per plate (50 mL of culture medium/225 cm² flask) and incubated in a CO₂
1144 incubator (37°C) for 7 days. Then, cells are divided for calculating the colony-
1145 forming capacity (abCE: absolute cloning efficiency) and the mutant frequency
1146 (MF: Mutant Frequency). For determining abCE, each cell suspension was
1147 diluted with culture medium and 200 cells per plate (5 mL of culture medium)
1148 were seeded into one 60 mm dia petri dish each and incubated for 7 days. The
1149 number of colonies counted, and abCE was calculated. For determining MF, the
1150 cell suspension was diluted with culture medium containing 6-TG (final 6-TG

1151 concentration: approximately 5 µg/mL) to 2×10^5 cells per plate (10 mL of culture
1152 medium), five 90 mm dia petri dishes each, and then selectively cultured for 11
1153 days. After the end of incubation, the number of colonies was counted and MF
1154 was calculated. These tests were performed by the Safety Research Institute for
1155 Chemical Compounds Co., Ltd. (Sapporo).
1156

1157 **Figure S1. Identification and cytotoxicity of s2U.**

1158 **A**, Schematic representation of the compound screening using BHK-21 cells and
1159 flaviviruses. **B**, Screening results of s2U. Antiviral assays were carried out as
1160 described in Supplementary Table S3. EC₅₀ (50% effective concentration) values
1161 represent mean values (n = 2). **C**, Effect of s2U on cell proliferation. Cells were
1162 incubated with serial dilutions of the compound. Resazurin reduction assay or
1163 CellTiter-Glo assay was performed at 3- or 4-days post-treatment. Cytotoxicity
1164 (%) is expressed relative to the values for the DMSO-treated samples and cell-
1165 free samples. The EC₅₀ and CC₅₀ (50% cytotoxic concentration) values were
1166 defined in GraphPad Prism versions 8.4.3 and 9.5.1 with a variable slope (four
1167 parameters).

1168

1169 **Figure S2. Dose-response inhibition of several RNA viruses by s2U.**

1170 Cells were infected with DENV2 (multiplicity of infection [MOI] = 0.05), ZIKV (MOI
1171 = 0.05), YFV (MOI = 0.05), JEV (MOI = 0.05), WNV (MOI = 0.05), CHIKV (MOI =
1172 0.01), HCoV-229E (MOI = 0.005), HCoV-OC43 (MOI = 0.1), SARS-CoV (MOI =
1173 0.01), MERS-CoV (MOI = 0.01) and several SARS-CoV-2 variants (MOI = 0.01)
1174 containing a serially diluted compound. Cell lysates were collected for viral RNA
1175 determination, and viral RNA levels were determined relative to *ACTB* transcripts.
1176 The 50% and 90% effective concentration (EC₅₀ and EC₉₀) values were defined
1177 in GraphPad Prism versions 8.4.3 and 9.5.1 with a variable slope (Find
1178 ECanything; F = 90). Data are presented as mean values of biological triplicates
1179 from one of the experiments, and error bars indicate SD.

1180

1181 **Figure S3. Antiviral activity of s2U against several RNA and DNA viruses.**

1182 **A**, Dose-response inhibition of viral protein expression in the HCoV-OC43-
1183 infected cells. Cells were stained with viral-specific antibodies (green,
1184 Nucleocapsid) and counterstained with Hoechst 33342 nuclear dye (blue). Scale
1185 bars indicate 200 μm. **B–E**, Dose-response inhibition of SARS-CoV-2
1186 propagation by s2U. Supernatants of SARS-CoV-2-infected VeroE6/TMPRSS2
1187 (**B**), VeroE6/ACE2/TMPRSS2 (**C**), and A549/ACE2/TMPRSS2 (**D**, **E**) cells were
1188 collected at 24- (**A**) or 48- (**C–E**) hours post-infection (hpi), and dilutions were
1189 used to inoculate VeroE6/ACE2/TMPRSS2 cells. Two days after inoculation, viral
1190 titers were determined by plaque assay. **F**, **G**, s2U did not inhibit RABV (**F**) and
1191 RVFV (**G**) virus replication. Cell lysates were collected for viral RNA
1192 determination; viral RNA levels were determined relative to *ACTB* or *18S rRNA*
1193 transcripts. **H**, s2U did not inhibit HSV-1 virus replication. Cell lysates were
1194 collected for viral DNA determination; viral DNA levels were determined relative
1195 to *ACTB* transcripts. Data are presented as mean values of biological triplicates
1196 from one of the experiments, and error bars indicate standard deviation (SD).
1197 Statistically significant differences were determined using a one-way ANOVA

1198 followed by Dunnett's multiple comparisons test to compare with non-treated
1199 cells; * $p < 0.01$, ** $p < 0.005$, *** $p < 0.0005$, and **** $p < 0.0001$.

1200

1201 **Figure S4. Molecular target and mechanism of action of s2U.**

1202 **A**, Ribonucleotide competition for HCoV-229E inhibition by s2U. HCoV-229E
1203 (MOI = 0.005)-infected MRC5 cells were treated with 15 μ M of s2U and serial
1204 dilutions of exogenous nucleosides. A resazurin reduction assay was performed
1205 at 3 days post-infection (dpi). Antiviral activities (%) are expressed relative to the
1206 values for the DMSO-treated, infected samples and non-infected samples. **B, C**,
1207 Effect of s2U resistance mutation on replication fitness. BHK-21 (**B**) and VeroE6
1208 (**C**) cells were infected with rgDENV2-WT or rgDENV2-NS5-G605V (MOI = 0.01)
1209 for 1 h. Cell lysates were collected at 24, 48, 72, and 96 hpi, and viral RNA levels
1210 were determined relative to *18S rRNA* (BHK-21) or *ACTB* (VeroE6) transcripts.
1211 Data are presented as mean values, and error bars indicate SD. Statistically
1212 significant differences between wildtype and G605V viruses (**B–C**) were
1213 determined using a two-way ANOVA followed by Bonferroni's multiple
1214 comparisons tests; * $p < 0.01$, ** $p < 0.005$, *** $p < 0.0005$, and **** $p < 0.0001$.

1215

1216 **Figure S5. Effect of s2U on mitochondrial biogenesis.**

1217 **A–D**, HepG2 cells were assayed for a reduction in mitochondrial-encoded protein
1218 COX-I or nuclear-encoded protein SDH-A after 5 days of incubation with 3-fold
1219 serial dilutions of s2U (**A**), ribavirin (**B**), favipiravir (**C**) and chloramphenicol (**D**).
1220 Inhibitory effects (% of Control) are expressed relative to the values for the
1221 DMSO-treated samples. **D**, 50% inhibitory concentration (IC_{50}) values of these
1222 compounds against protein expression. The IC_{50} value was defined in GraphPad
1223 Prism version 8.4.3 with a variable slope (four parameters).

1224

1225 **Figure S6. Establishment of mouse-adapted DENV2 strain (DENV2 AG-P10).**

1226 **A**, Schematic representation of the passage history of DENV2 in AG129 mice.
1227 Virus in serum from infected mice was propagated in C6/36 cells. **B**, Survival of
1228 DENV2 AG-P10-infected AG129 mice. Mice were intraperitoneally inoculated
1229 with 4×10^5 plaque-forming units [PFU] of a DENV2 clinical isolate ($n = 3$) and
1230 DENV2 AG-P10 ($n = 5$). Survival was monitored daily. **C**, Viral RNA copies/mL in
1231 organ samples were quantified using qRT-PCR. At 4 dpi, the infected mice ($1 \times$
1232 10^3 PFU of DENV2 AG-P10, $n = 2$) were euthanized under deep anesthesia by
1233 isoflurane inhalation, and serum and whole tissues (spleen, kidney, liver, small
1234 intestine, large intestine, and brain) were harvested and homogenized in PBS
1235 with a TissueRuptor. **D**, Amino acid substitutions occurred during the passage.
1236 Data are presented as mean values, and error bars indicate SD.

1237

1238 **Figure S7. Establishment of mouse-adapted SARS-CoV-2 strain (SARS-**
1239 **CoV-2 MA-P10).**

1240 **A**, Schematic representation of the passage history of SARS-CoV-2 in BALB/c
1241 mice. **B**, Virus titers in lung homogenates from SARS-CoV-2-infected mice from
1242 passage 1 (P1) to P10 (n = 3–9). **C**, Survival of SARS-CoV-2 MA-P10-infected
1243 BALB/c mice. Young (5-week-old) and adult (30–50-week-old) female mice were
1244 intranasally inoculated with 2×10^5 TCID₅₀ of SARS-CoV-2 MA-P10 (n = 5 per
1245 group). Survival was monitored daily. **D**, **E**, Virus titers and viral RNA loads in
1246 lung from SARS-CoV-2-MA-P10-infected mice. Virus titers (**D**) were quantified by
1247 a standard 50% tissue culture infection dose (TCID₅₀) assay using
1248 VeroE6/TMPRSS2 cells. Viral RNA copies/mL (**E**) were quantified using qRT-
1249 PCR. **F**, Macroscopic appearance of lung tissue of SARS-CoV-2-MA-P10-
1250 infected mice at 1, 3, and 5 dpi. **G**, Amino acid substitutions occurred during the
1251 passage. Data are presented as mean values, and error bars indicate SD.

1252

1253 **Figure S8. In vivo efficacy of s2U in the DENV2 and SARS-CoV-2 mouse**
1254 **model.**

1255 **A**, Schematic representation of the viremia study using AG129 mice and strain
1256 DENV2 AG-P10. **B–D**, Effect of s2U on viremia at 3 dpi in mice treated twice daily
1257 with s2U (50 or 150 mg/kg) compared with vehicle-treated mice (n = 5 per group).
1258 The relative viral RNA level (DENV2 copies/18S copies) of spleen (**B**), kidney (**C**),
1259 and liver (**D**) samples were quantified using qRT-PCR. **E**, Schematic
1260 representation of the study using BALB/c mice and SARS-CoV-2 MA-P10. **F–H**,
1261 Relative *Ifnb* (**F**), *Il6* (**G**), and *Cxcl10* (**H**) gene expression profiles in lungs from
1262 mice at 1 dpi with SARS-CoV-2. Cytokine RNA levels were determined relative
1263 to *18S rRNA* transcripts. **I**, Schematic representation of the viremia study using
1264 BALB/c mice and SARS-CoV-2 MA-P10. **J**, Effect of s2U on viremia at 1 dpi in
1265 mice orally administered 300 mg/kg s2U twice daily compared with vehicle-
1266 treated mice (n = 5 per group). Virus titers in lung samples were quantified by a
1267 standard TCID₅₀ assay using VeroE6/TMPRSS2 cells. Data are presented as
1268 mean values, and error bars indicate SD. Statistically significant differences
1269 between the s2U-treated and vehicle-treated groups were determined using a
1270 one-way ANOVA followed by Dunnett's multiple comparisons tests (**B–D**, **F–H**)
1271 or unpaired *t*-test (**J**); * $p < 0.01$, ** $p < 0.005$, *** $p < 0.0005$, and **** $p <$
1272 0.0001 .

1273

1274 **Figure S9. Close-up view of the catalytic site including the escape mutation**
1275 **site, residue 605, in crystal structures of DENV and SARS-CoV-2 RdRps.**
1276 **These are superimposed into MNV RdRp complexed with s2U.**

1277 G605 in motif B (left bottom and right) and located close to the active site, D663
1278 in motif C, a catalytic region in DENV RdRp. The crystal structure of DENV RdRp
1279 showed the disordered region for residues 602-605 (cyan). s2U (white) binds to
1280 D346 of MNV RdRp, which corresponds to D663 in DENV and D760 in SARS-
1281 CoV-2. This residue is conserved in a wide range of viruses. s2U also binds to
1282 another catalytic residue D250, which corresponds to D539 in DENV and D623
1283 in SARS-CoV-2. This residue is conserved in positive-sense RNA viruses but not
1284 in negative-sense RNA viruses.

1285

1286 **Figure S10. Pharmacokinetic (PK) properties of s2U.**

1287 **A**, *In vitro* absorption, distribution, metabolism, and excretion (ADME) properties
1288 of s2U. **B–D**, Pharmacokinetic properties of s2U in mice after oral (**B**) and
1289 intravenous (**C**) dosing. s2U was administered to 5-week-old female BALB/c mice
1290 (n = 3 per group) *via* oral gavage as a solution formulated in 5% DMSO/0.5%
1291 methylcellulose at 150 mg/kg or intravenously as a saline solution at 20 mg/kg.
1292 C_0 : initial concentration, C_{max} : maximum plasma concentration, T_{max} : time to
1293 reach C_{max} , $t_{1/2}$: terminal phase elimination half-life, AUC: area under the plasma
1294 concentration versus the time, AUC_{∞} : AUC curve to infinite time, CL_{tot} : total
1295 clearance, V_{dz} : volume of distribution at the terminal phase, BA (F): bioavailability.
1296 **E, F**, Simulation of twice-daily or once-daily doses of s2U by oral or intravenous
1297 administration derived from the single-dose PK experiment. Data are presented
1298 as mean values, and error bars indicate SD (**B, C**).

1299

1300 **Figure S11. *In vivo* toxicity evaluation of s2U using BALB/c mice.**

1301 *In vivo* toxicity evaluation of s2U in mice after oral and intravenous dosing. s2U
1302 was administered to 5-week-old female BALB/c mice (n = 3 or 5 per group) *via*
1303 oral gavage (PO) as a solution formulated in 5% DMSO/0.5% methylcellulose at
1304 150 or 300 mg/kg or intravenously (IV) as a saline solution at 25 or 50 mg/kg.
1305 Body weight changes were monitored daily for 7 days. Data are presented as
1306 mean values, and error bars indicate SD.

1307

1308 **Table S1. Antiviral activity of reference compounds against various RNA**
1309 **viruses.**

1310 Antiviral assays were carried out as described in Supplementary Table S3 and
1311 S4. EC₅₀: 50% effective concentration. EC₉₀: 90% effective concentration.

1312 a: EC₅₀ values represent mean values from at least three independently
1313 performed experiments (n = 2).

1314 b: EC₉₀ values represent mean values from a single experiment with biological
1315 triplicates.

1316 c: Fold change is calculated from the ratio of rgNS5-G605V/rgWT.

1317

1318

1319 **Table S2. Bacterial reverse mutation test and *in vitro* gene mutation test**
1320 **using the *Hprt* genes in V79 cells.**

1321

1322

1323 **Table S3. *In vitro* assay conditions (CPE-based assay).**

1324

1325

1326 **Table S4. *In vitro* assay conditions (qPCR assay, IFA, and Plaque assay).**

1327

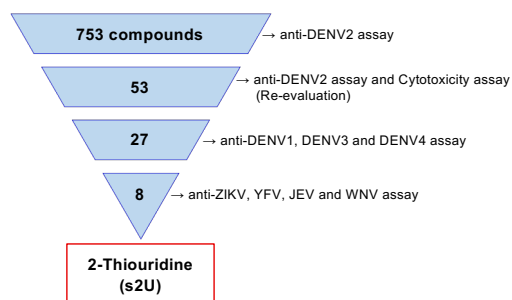
1328

1329 **Table S5. Sequence of primers and probes for the qPCR assays.**

1330

Figure S1

A



B

| Screening Results | | | |
|-------------------|----------------------|--------|-----------------------|
| Virus | Strain | Cell | EC ₅₀ (μM) |
| DENV1 | D1/hu/PHL/10-07 | BHK-21 | 2.6 |
| DENV2 | D2/hu/INDIA/09-74 | BHK-21 | 0.58 |
| DENV3 | D3/hu/Thailand/00-40 | BHK-21 | 2.1 |
| DENV4 | D4/hu/Solomon/09-11 | BHK-21 | 1.8 |
| ZIKV | MR766 | BHK-21 | 5.0 |
| YFV | 17D-204 | BHK-21 | 2.9 |
| JEV | Beijing-1 | BHK-21 | 4.8 |
| WNV | NY99 | BHK-21 | 5.3 |

C

| Cell | Species | Organ | CC ₅₀ (μM) ^a |
|--------------------|---------|----------|------------------------------------|
| BHK-21 | Hamster | Kidney | > 400 ^{b,c} |
| VeroE6 | Monkey | Kidney | > 400 ^{b,c} |
| VeroE6/ TMPRSS2 | Monkey | Kidney | 282.8 ^b |
| MRC5 | Human | Lung | > 400 ^b |
| 293T | Human | Kidney | 100.6 ^c |
| Huh7 | Human | Liver | > 400 ^b |
| MOLT4 | Human | T cell | > 50 ^c |
| THP-1 | Human | Monocyte | > 50 ^c |

a : CC₅₀ values represent mean values from at least three independently performed experiments (n = 2).

b : CellTiter-Glo assay

c : Resazurin assay

Figure S2

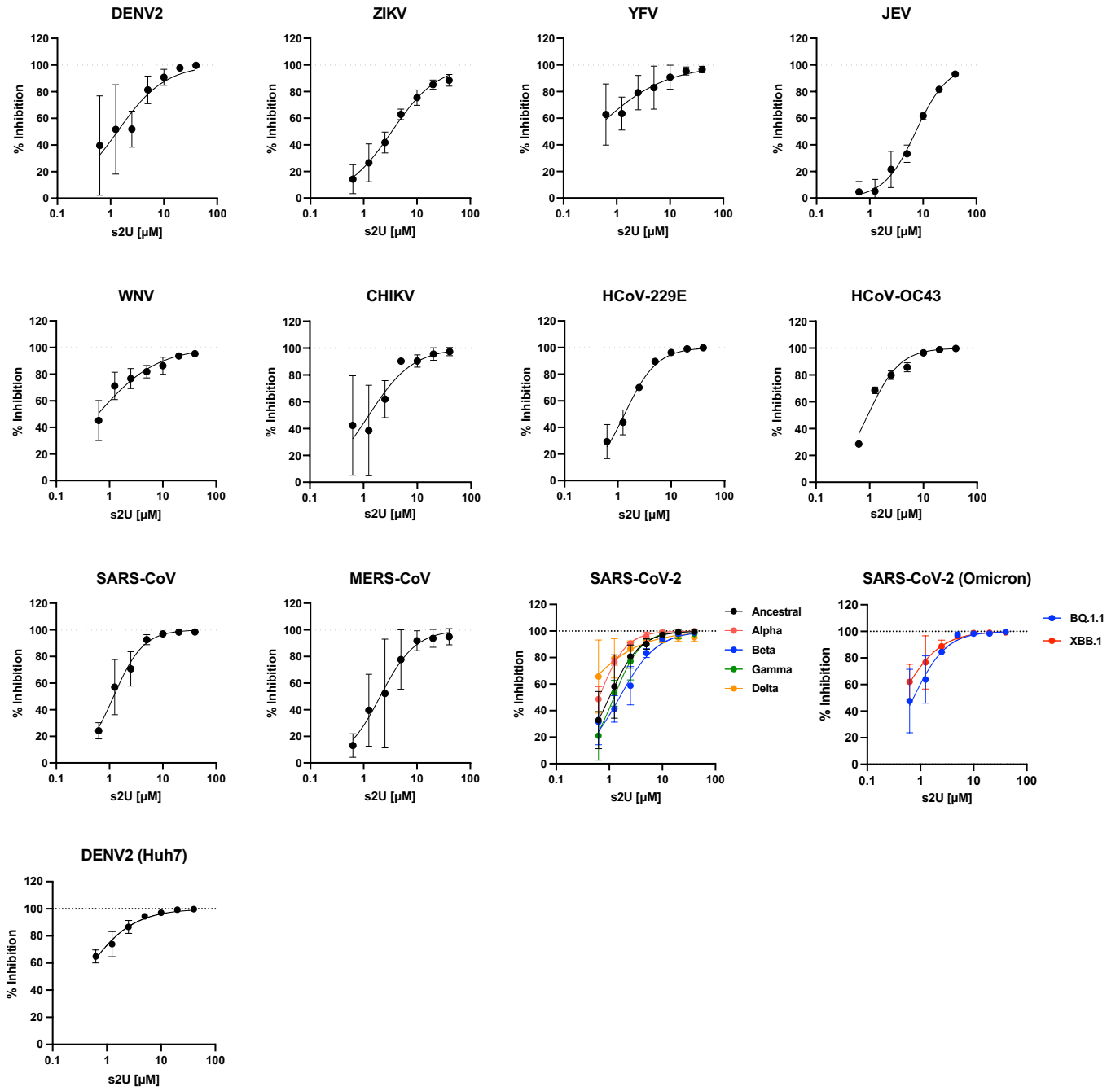
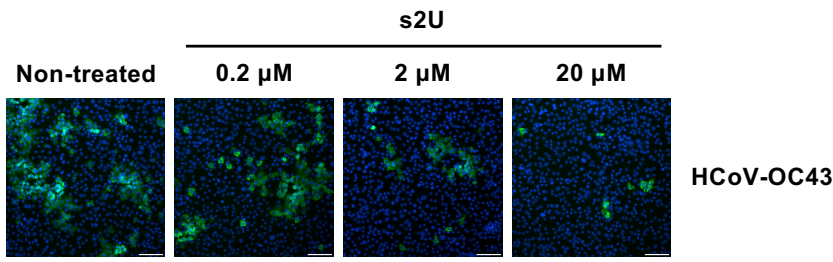
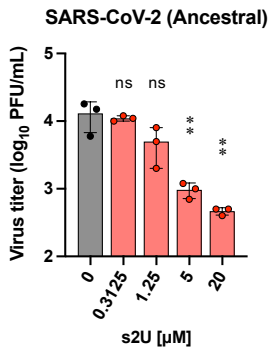


Figure S3

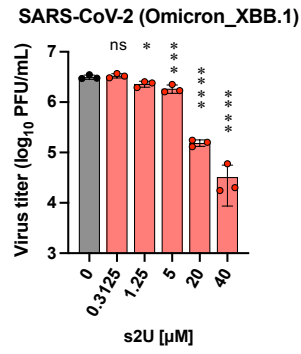
A



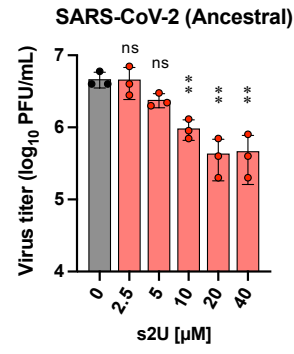
B



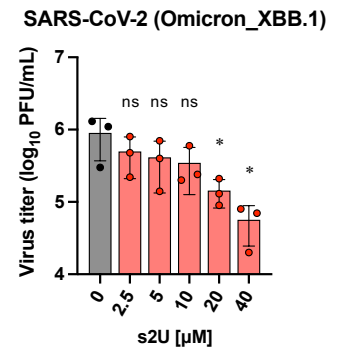
C



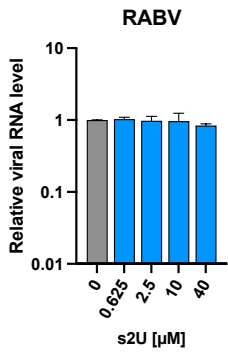
D



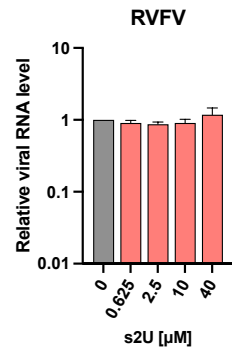
E



F



G



H

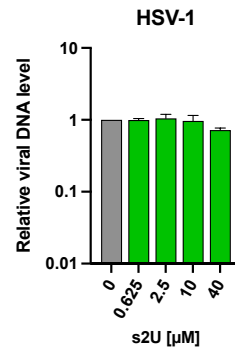
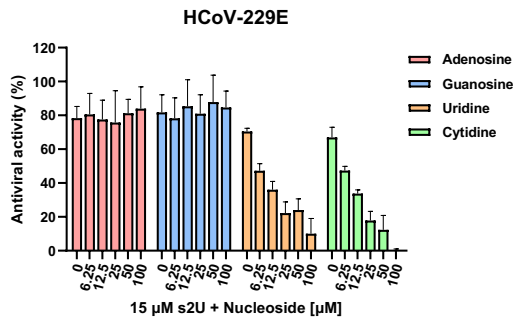
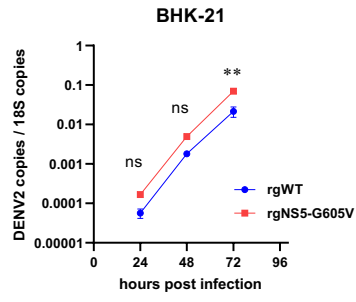


Figure S4

A



B



C

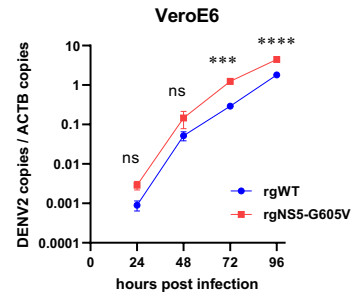
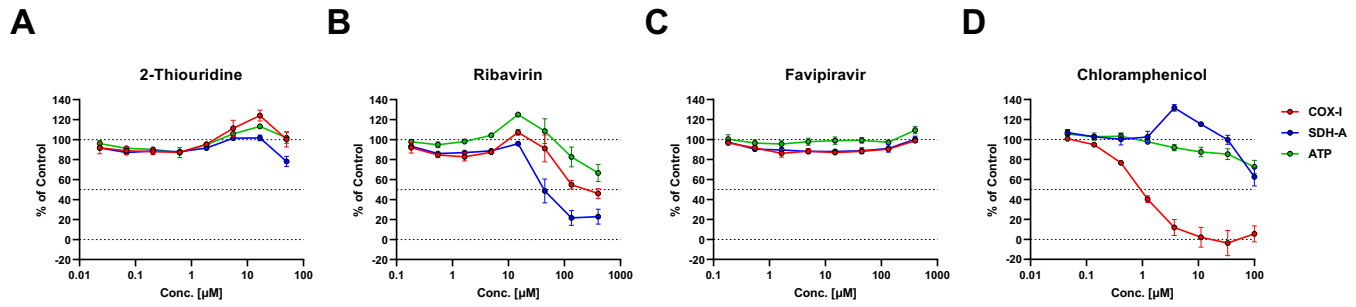


Figure S5



E

| Protein | IC ₅₀ (μM) ^a | | | |
|--------------------|------------------------------------|-----------|-------------|------------------------------|
| | 2-Thiouridine | Ribavirin | Favipiravir | Chloramphenicol ^e |
| COX-I ^b | >50 | 97 ± 33 | >400 | 0.97 ± 0.060 |
| SDH-A ^c | >50 | 45 ± 1.4 | >400 | >100 |
| ATP ^d | >50 | >400 | >400 | >100 |

a : IC₅₀ values represent mean values ± SEM from three independently performed experiments (n = 2).

b : Cytochrome c oxidase (COX-I) is the mitochondrial DNA-encoded protein.

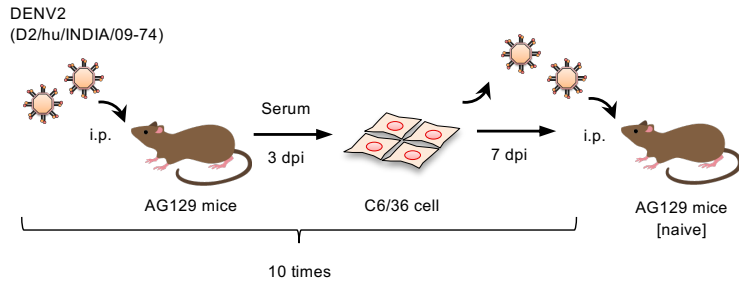
c : Succinate dehydrogenase A subunit (SDH-A) is the nuclear DNA-encoded protein.

d : Cell viability monitored as ATP level was measured using Cell-Titer Glo® 2.0 Assay.

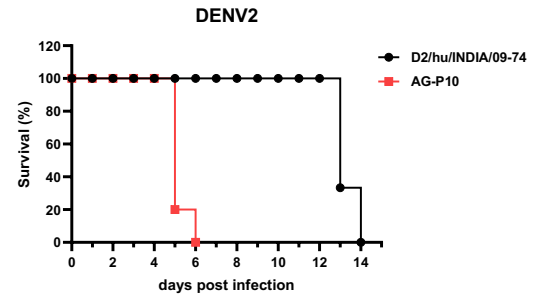
e : Chloramphenicol was used as control compound for specific inhibition of COX-I synthesis.

Figure S6

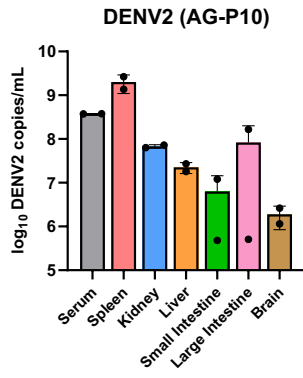
A



B



C

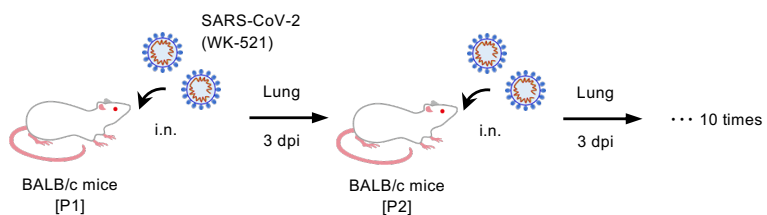


D

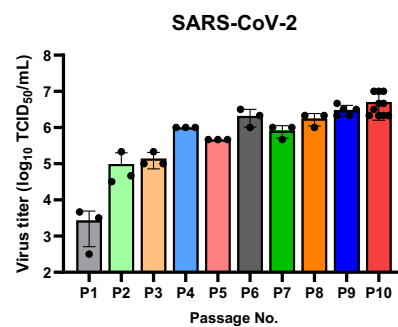
| | | |
|-------------------------|-------|-------|
| Viral protein | NS4B | NS5 |
| Amino acid substitution | A119T | E802Q |

Figure S7

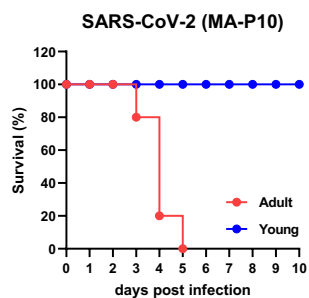
A



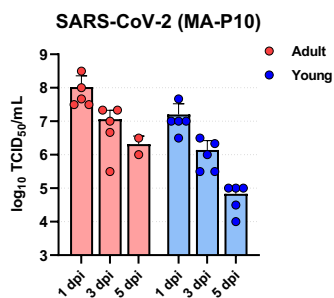
B



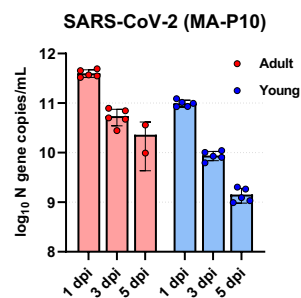
C



D



E



F

| Group | 1 dpi | 3 dpi | 5 dpi |
|-------------------|-------|-------|-------|
| Young (5 wks) | | | |
| Adult (35-45 wks) | | | dead |

G

| Viral protein | Amino acid substitution |
|---------------|-------------------------|
| nsp4 | A457V |
| nsp5 | E270G |
| nsp9 | R39K |
| nsp16 | K160R |
| Spike | Q498H |
| Nucleocapsid | T205I |

Figure S8

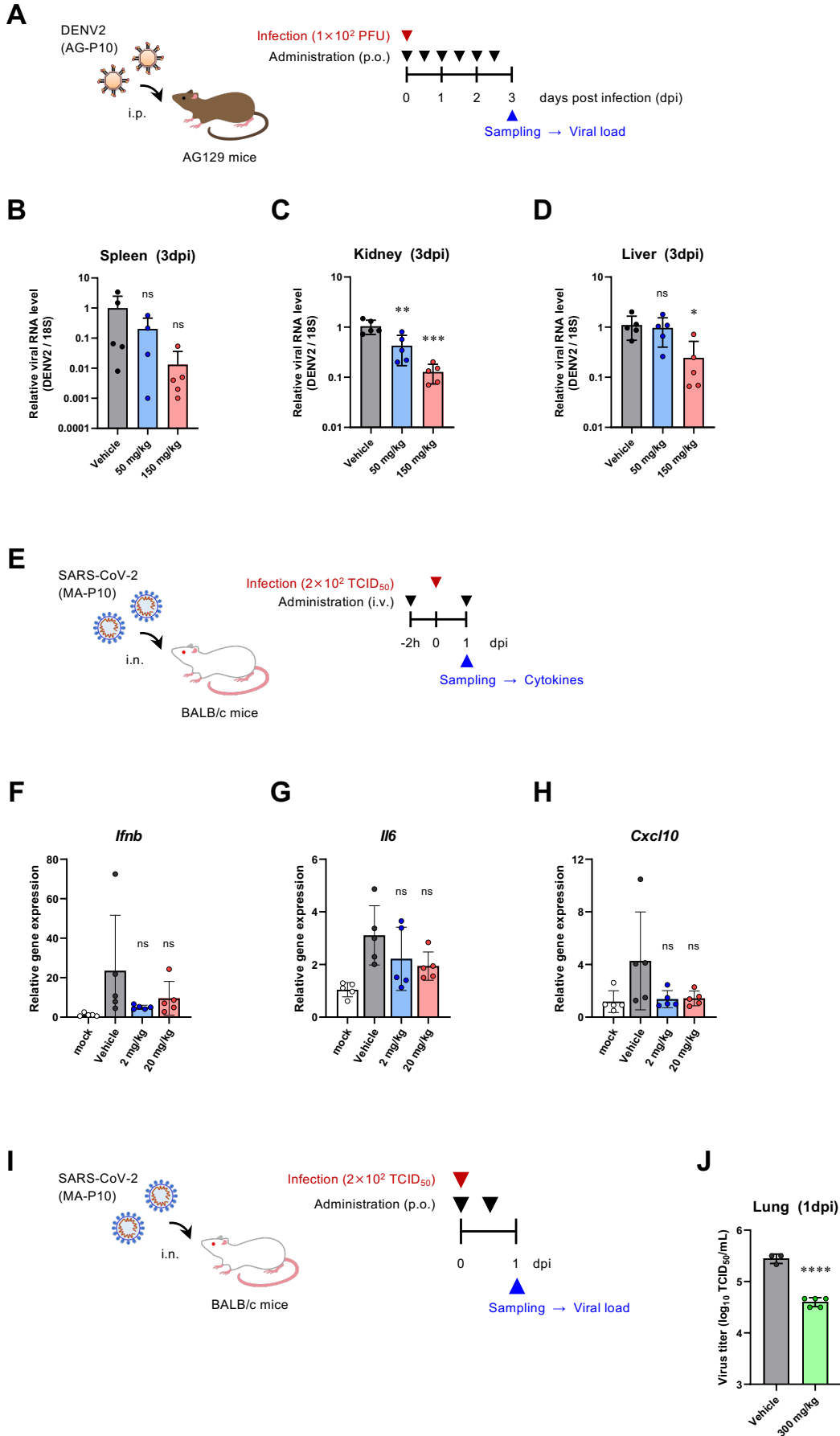


Figure S9

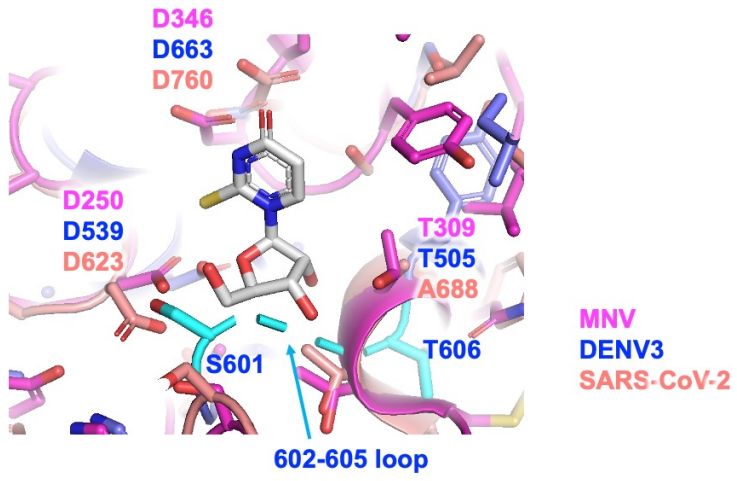
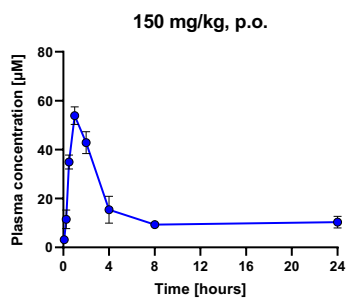


Figure S10

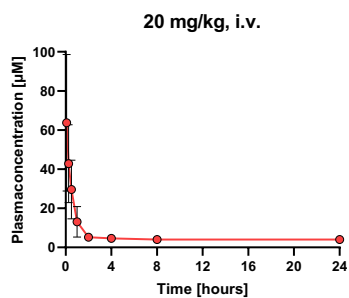
A

| Compound | Solubility (μM) | | Membrane Permeability ($\times 10^{-6}$ cm/sec) | Metabolic stability (mL/min/kg) | | Protein binding (Unbound fraction) | |
|---------------|------------------------------|-------------|--|--|--|------------------------------------|--------------|
| | JP1 (pH1.2) | JP2 (pH6.8) | PAMPA (pH6.5) | Human liver microsome | Mouse liver microsome | Human plasma | Mouse plasma |
| 2-Thiouridine | 78 | >100 | 0.013 | <22.0 ($<17.6\mu\text{L}/\text{min}/\text{mg}$) | <69.8 ($<17.6\mu\text{L}/\text{min}/\text{mg}$) | 0.70 | 0.73 |

B



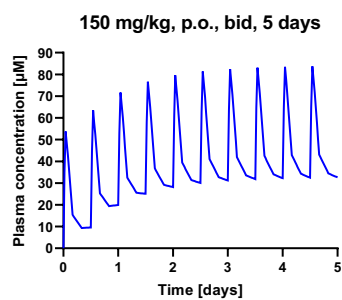
C



D

| Compound | Route | Dose (mg/kg) | C_0 ($\mu\text{g}/\text{mL}$) | C_{max} ($\mu\text{g}/\text{mL}$) | T_{max} (hr) | $t_{1/2}$ (hr) | AUC_{∞} ($\mu\text{g}/\text{mL}\cdot\text{hr}$) | CL_{tot} or CL_{tot}/F (mL/hr/kg) | V_{dz} or V_{dz}/F (mL/kg) | BA (F) (%) |
|---------------|-------|--------------|-----------------------------------|--|-----------------------|----------------|---|---|--|------------|
| 2-Thiouridine | p.o. | 150 | | 14.0 | 1 | 31.2 | 198 | 757 | 34025 | 17.3 |
| | i.v. | 20 | 20 | | | 80.7 | 153 | 131.1 | 15260 | |

E



F

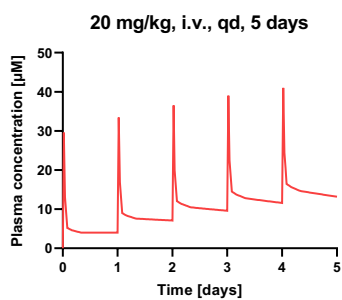


Figure S11

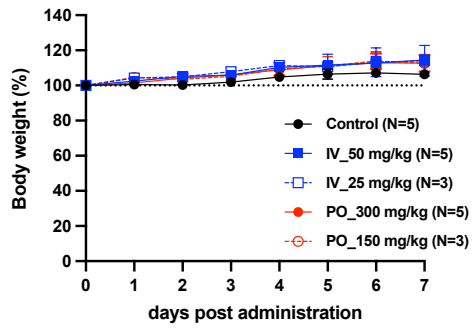


Table S1

| MTT / Resazurin Assay Results | | | EC₅₀ (μM)^a | | | |
|--------------------------------------|---------------------------|----------------|---|-------------|--------------------------------|-------------|
| Virus | Strain | Cell | Ribavirin | Favipiravir | Remdesivir | GS-441524 |
| DENV1 | D1/hu/PHL/10-07 | BHK-21 | 46 | 18 | | |
| DENV2 | D2/hu/INDIA/09-74 | BHK-21 | 32 | 20 | | |
| | AG-P10 (Mouse-adapted) | BHK-21 | 77 | 16 | | |
| DENV3 | D3/hu/Thailand/00-40 | BHK-21 | 61 | 13 | | |
| DENV4 | D4/hu/Solomon/09-11 | BHK-21 | 91 | 5.2 | | |
| ZIKV | MR766 | BHK-21 | 18 | 39 | | |
| YFV | 17D-204 | BHK-21 | 15 | 24 | | |
| JEV | Beijing-1 | BHK-21 | 33 | 80 | | |
| WNV | NY99 | BHK-21 | 43 | 36 | | |
| CHIKV | SL10571 | BHK-21 | 46 | 8.1 | | |
| HCoV | 229E | MRC5 | | | 0.071 | 0.76 |
| HCoV | OC43 | MRC5 | | | 0.23 | 2.0 |
| SARS-CoV-2 | WK-521 (Ancestral) | VeroE6/TMPRSS2 | | | 1.5 | |
| | QK002 (Alpha) | VeroE6/TMPRSS2 | | | 2.0 | |
| | TY8-612 (Beta) | VeroE6/TMPRSS2 | | | 0.91 | |
| | TY7-501 (Gamma) | VeroE6/TMPRSS2 | | | 0.91 | |
| | TY11-927 (Delta) | VeroE6/TMPRSS2 | | | 1.7 | |
| | TY38-873 (Omicron BA.1) | VeroE6/TMPRSS2 | | | 0.67 | |
| | TY40-385 (Omicron BA.2) | VeroE6/TMPRSS2 | | | 1.1 | |
| | TY41-703 (Omicron BA.4) | VeroE6/TMPRSS2 | | | 0.77 | |
| | TY41-702 (Omicron BA.5) | VeroE6/TMPRSS2 | | | 1.0 | |
| | TY41-796 (Omicron_BQ.1.1) | VeroE6/TMPRSS2 | | | 1.2 | |
| | TY41-795 (Omicron_XBB.1) | VeroE6/TMPRSS2 | | | 0.78 | |
| MA-P10 (Mouse-adapted) | VeroE6/TMPRSS2 | | | 1.3 | | |
| RABV | HEP | BHK-21 | 16 | 5.9 | | |
| LACV | ATCC VR-1834 | MDBK | 2.5 | 20 | | |
| LPHV | 11SB17 | KB | 5.3 | >100 | | |
| LCMV | Armstrong | KB | 1.8 | 21 | | |
| JUNV | Candid #1 | 293T | 2.6 | 10 | | |
| SFTSV | ArtLN/2017 | MDCK | 5.4 | 7.3 | | |
| RVFV | MP12 | MDCK | 17 | 21 | | |
| TPMV | VRC-66412 | VeroE6 | 6.7 | 31 | | |
| IAV H5N1 | A/Hong Kong/483/97 | A549 | 26 | 6.2 | | |
| IAV H7N9 | A/Anhui/1/2013 | MA104/TMPRSS2 | 3.7 | 12 | | |
| Resazurin Assay Results | | | EC₅₀ (μM)^a | | Fold change^c | |
| Virus | Strain | Cell | Ribavirin | Favipiravir | Ribavirin | Favipiravir |
| rgDENV2 | Wild type | BHK-21 | 16 | 7.9 | | |
| rgDENV2 | NS5-G605V | BHK-21 | 37 | 17 | 2.3 | 2.2 |
| qRT-PCR Assay Results | | | EC₉₀ (μM)^b | | | |
| Virus | Strain | Cell | Remdesivir | | | |
| SARS-CoV | Hanoi | VeroE6 | 2.7 | | | |
| SARS-CoV-2 | WK-521 (Ancestral) | VeroE6/TMPRSS2 | 3.3 | | | |

a : EC₅₀ values represent mean values from at least three independently performed experiments (n = 2).

b : EC₉₀ values represent mean values from a single experiment with biological triplicates.

c : Fold change is calculated from the ratio of rgNS5-G605V/rgWT.

Table S2

| Bacterial reverse mutation test of s2U | | | | | | | |
|---|--------------------|---------------------------------|--|--------------|---------------|--------------|--------------|
| | | dose $\mu\text{g}/\text{plate}$ | Number of revertants/plate (Mean \pm SD) | | | | |
| | | | TA100 | TA1535 | WPuvrA | TA98 | TA1537 |
| S9 mix (-) | s2U | 0 | 115 \pm 17 | 11 \pm 2 | 23 \pm 5 | 16 \pm 3 | 6 \pm 1 |
| | | 1,667 | 112 \pm 11 | 6 \pm 1 | 27 \pm 6 | 19 \pm 1 | 8 \pm 1 |
| | | 5,000 | 98 \pm 2 | 10 \pm 1 | 28 \pm 2 | 11 \pm 4 | 4 \pm 1 |
| S9 mix (+) | s2U | 0 | 115 \pm 17 | 14 \pm 3 | 24 \pm 3 | 24 \pm 3 | 12 \pm 1 |
| | | 1,667 | 126 \pm 6 | 11 \pm 4 | 34 \pm 6 | 37 \pm 4 | 8 \pm 2 |
| | | 5,000 | 119 \pm 8 | 11 \pm 4 | 29 \pm 2 | 13 \pm 1 | 5 \pm 1 |
| S9 mix (-) | AF2 ^{*a} | ^{*b} | 714 \pm 31 | | 102 \pm 6 | 294 \pm 4 | |
| | NaN ₃ | 0.5 | | 432 \pm 76 | | | |
| | 9-AA ^{*a} | 80 | | | | | 546 \pm 19 |
| S9 mix (+) | 2-AA ^{*a} | ^{*c} | 1441 \pm 89 | 326 \pm 33 | 1158 \pm 76 | 424 \pm 30 | 241 \pm 20 |

***In vitro* gene mutation test of s2U using the Hprt genes in V79 cells**

| | | dose $\mu\text{g}/\text{ml}$ | relative cell survival (%) | mutation frequency ($\times 10^{-6}$) ^{*d} |
|------------|-------------------|------------------------------|----------------------------|---|
| S9 mix (-) | s2U | 0 | 100 | 12.72 |
| | | 51.6 | 107 | 10.84 |
| | | 77.3 | 107 | 10.11 |
| | | 116 | 87 | 11.11 |
| | | 174 | 102 | 14.94 |
| | | 261 | 76 | 17.44 |
| S9 mix (+) | s2U | 0 | 100 | 9.95 |
| | | 51.6 | 103 | 11.37 |
| | | 77.3 | 121 | 12.31 |
| | | 116 | 95 | 11.65 |
| | | 174 | 86 | 10.89 |
| | | 261 | 99 | 15.96 |
| S9 mix (+) | 3MC ^{*e} | 5 | 77 | 598.74 |

*a : positive control: AF-2: 2-(2-furyl)-3-(5-nitro-2-furyl)-acrylamide, 9-AA: 9-aminoacridine, 2-AA: 2-aminoanthracene .

*b : AF2 conc ($\mu\text{g}/\text{plate}$): 0.01 (TA100), 0.01 (WPuvrA), 0.1 (TA98).

*c : 2AA conc ($\mu\text{g}/\text{plate}$): 1 (TA100), 2 (TA1535), 10 (WPuvrA), 0.5 (TA98), 2 (TA1537).

*d : MF is determined as; [total of the number of mutant colonies / (abCE \times total of the number of seeding cells)], where abCE is determined as the ratio of the number of colonies to the number of cells inoculated after phenotypic expression period.

*e : 3MC (3-methylcholanthrene).

Table S3

| MTT / Resazurin Assay | | | | | |
|-----------------------|---------------------------|----------------|-----------------------|-----------|--------|
| Virus | Strain | Cell | MOI | Method | Period |
| DENV1 | D1/hu/PHL/10-07 | BHK-21 | 10 TCID ₅₀ | Resazurin | 5 days |
| DENV2 | D2/hu/INDIA/09-74 | BHK-21 | MOI=0.01 | Resazurin | 4 days |
| | AG-P10 (Mouse-adapted) | BHK-21 | MOI=0.01 | Resazurin | 4 days |
| DENV3 | D3/hu/Thailand/00-40 | BHK-21 | 10 TCID ₅₀ | Resazurin | 5 days |
| DENV4 | D4/hu/Solomon/09-11 | BHK-21 | 10 TCID ₅₀ | Resazurin | 5 days |
| ZIKV | MR766 | BHK-21 | MOI=0.01 | MTT | 3 days |
| YFV | 17D-204 | BHK-21 | MOI=0.01 | MTT | 3 days |
| JEV | Beijing-1 | BHK-21 | 10 TCID ₅₀ | MTT | 3 days |
| | | VeroE6 | MOI=0.01 | MTT | |
| WNV | NY99 | BHK-21 | 10 TCID ₅₀ | MTT | 3 days |
| | | VeroE6 | MOI=0.01 | MTT | |
| CHIKV | SL10571 | BHK-21 | 10 TCID ₅₀ | MTT | 3 days |
| | | VeroE6 | MOI=0.01 | MTT | |
| HCoV | 229E | MRC5 | MOI=0.005 | Resazurin | 3 days |
| HCoV | OC43 | MRC5 | MOI=0.01 | Resazurin | 3 days |
| SARS-CoV-2 | WK-521 (Ancestral) | VeroE6/TMPRSS2 | 10 TCID ₅₀ | MTT | 2 days |
| | QK002 (Alpha) | VeroE6/TMPRSS2 | 10 TCID ₅₀ | MTT | 2 days |
| | TY8-612 (Beta) | VeroE6/TMPRSS2 | 10 TCID ₅₀ | MTT | 2 days |
| | TY7-501 (Gamma) | VeroE6/TMPRSS2 | 10 TCID ₅₀ | MTT | 2 days |
| | TY11-927 (Delta) | VeroE6/TMPRSS2 | 10 TCID ₅₀ | MTT | 2 days |
| | TY38-873 (Omicron BA.1) | VeroE6/TMPRSS2 | 10 TCID ₅₀ | MTT | 3 days |
| | TY40-385 (Omicron BA.2) | VeroE6/TMPRSS2 | 10 TCID ₅₀ | MTT | 3 days |
| | TY41-703 (Omicron BA.4) | VeroE6/TMPRSS2 | 10 TCID ₅₀ | MTT | 3 days |
| | TY41-702 (Omicron BA.5) | VeroE6/TMPRSS2 | 10 TCID ₅₀ | MTT | 3 days |
| | TY41-796 (Omicron_BQ.1.1) | VeroE6/TMPRSS2 | 10 TCID ₅₀ | MTT | 2 days |
| | TY41-795 (Omicron_XBB.1) | VeroE6/TMPRSS2 | 10 TCID ₅₀ | MTT | 3 days |
| | MA-P10 (Mouse-adapted) | VeroE6/TMPRSS2 | 10 TCID ₅₀ | MTT | 2 days |
| RABV | HEP | BHK-21 | 10 TCID ₅₀ | MTT | 3 days |
| LACV | ATCC VR-1834 | MDBK | 10 TCID ₅₀ | MTT | 3 days |
| LPHV | 11SB17 | KB | 10 TCID ₅₀ | MTT | 4 days |
| LCMV | Armstrong | KB | 10 TCID ₅₀ | MTT | 4 days |
| JUNV | Candid #1 | 293T | 10 TCID ₅₀ | MTT | 4 days |
| SFTSV | ArtLN/2017 | MDCK | 10 TCID ₅₀ | MTT | 4 days |
| RVFV | MP12 | MDCK | 10 TCID ₅₀ | MTT | 3 days |
| TPMV | VRC-66412 | VeroE6 | 10 TCID ₅₀ | MTT | 4 days |
| IAV H5N1 | A/Hong Kong/483/97 | A549 | 10 TCID ₅₀ | MTT | 3 days |
| IAV H7N9 | A/Anhui/1/2013 | MA104/TMPRSS2 | 10 TCID ₅₀ | MTT | 3 days |
| rgDENV2 | Wild type | BHK-21 | MOI=0.1 | Resazurin | 4 days |
| rgDENV2 | NS5-G605V | BHK-21 | MOI=0.1 | Resazurin | 4 days |

Table S4

| qRT-PCR (qPCR) Assay | | | | | |
|-----------------------------|---------------------------|---------------------|--------------------|--------|------------------|
| Virus | Strain | Cell | MOI | Period | Internal control |
| DENV2 | D2/hu/INDIA/09-74 | VeroE6 | MOI=0.05 | 48 hpi | <i>ACTB</i> |
| | | Huh7 | MOI=0.05 | 48 hpi | <i>ACTB</i> |
| ZIKV | MR766 | VeroE6 | MOI=0.05 | 48 hpi | <i>ACTB</i> |
| YFV | 17D-204 | VeroE6 | MOI=0.05 | 48 hpi | <i>ACTB</i> |
| JEV | Beijing-1 | VeroE6 | MOI=0.01 | 48 hpi | <i>ACTB</i> |
| WNV | NY99 | VeroE6 | MOI=0.05 | 24 hpi | <i>ACTB</i> |
| CHIKV | SL10571 | VeroE6 | MOI=0.01 | 24 hpi | <i>ACTB</i> |
| HCoV | 229E | MRC5 | MOI=0.005 | 48 hpi | <i>ACTB</i> |
| HCoV | OC43 | VeroE6 | MOI=0.1 | 48 hpi | <i>ACTB</i> |
| SARS-CoV | Hanoi | VeroE6/TMPRSS2 | MOI=0.01 | 24 hpi | <i>ACTB</i> |
| SARS-CoV-2 | EMC2012 | VeroE6/TMPRSS2 | MOI=0.01 | 24 hpi | <i>ACTB</i> |
| | WK-521 (Ancestral) | VeroE6/TMPRSS2 | MOI=0.01 | 24 hpi | <i>ACTB</i> |
| | QK002 (Alpha) | VeroE6/TMPRSS2 | MOI=0.01 | 24 hpi | <i>ACTB</i> |
| | TY8-612 (Beta) | VeroE6/TMPRSS2 | MOI=0.01 | 24 hpi | <i>ACTB</i> |
| | TY7-501 (Gamma) | VeroE6/TMPRSS2 | MOI=0.01 | 24 hpi | <i>ACTB</i> |
| | TY11-927 (Delta) | VeroE6/TMPRSS2 | MOI=0.01 | 24 hpi | <i>ACTB</i> |
| | TY41-796 (Omicron_BQ.1.1) | VeroE6/ACE2/TMPRSS2 | MOI=0.01 | 24 hpi | <i>ACTB</i> |
| | TY41-795 (Omicron_XBB.1) | VeroE6/ACE2/TMPRSS2 | MOI=0.01 | 24 hpi | <i>ACTB</i> |
| RABV | HEP | BHK-21 | MOI=0.1 | 24 hpi | <i>18S rRNA</i> |
| RVFV | MP12 | VeroE6 | MOI=0.01 | 24 hpi | <i>ACTB</i> |
| HSV-1 | F | VeroE6 | MOI=0.1 | 24 hpi | <i>ACTB</i> |
| IFA | | | | | |
| Virus | Strain | Cell | MOI | Period | Antibody |
| DENV2 | D2/hu/INDIA/09-74 | VeroE6 | MOI=0.1 | 48 hpi | Envelope |
| CHIKV | SL10571 | VeroE6 | MOI=0.05 | 24 hpi | E1 |
| HCoV | OC43 | VeroE6/TMPRSS2 | MOI=0.1 | 48 hpi | Nucleocapsid |
| | WK-521 (Ancestral) | VeroE6/TMPRSS2 | MOI=0.005 | 24 hpi | Nucleocapsid |
| | TY41-796 (Omicron_BQ.1.1) | VeroE6/ACE2/TMPRSS2 | MOI=0.1 | 24 hpi | Nucleocapsid |
| | TY41-795 (Omicron_XBB.1) | VeroE6/ACE2/TMPRSS2 | MOI=0.1 | 24 hpi | Nucleocapsid |
| Plaque Assay | | | | | |
| Virus | Strain | Cell | Overlay | Period | |
| DENV2 | D2/hu/INDIA/09-74 | BHK-21 | 1% Methylcellulose | 4 days | |
| SARS-CoV-2 | WK-521 (Ancestral) | VeroE6/ACE2/TMPRSS2 | 0.5% Agar | 2 days | |
| | TY41-795 (Omicron_XBB.1) | VeroE6/ACE2/TMPRSS2 | 0.5% Agar | 2 days | |

Table S5

| Virus | | Sequence (5'→3') |
|-------------------------------|----|--|
| DENV2 | Fw | AGTGGACACGAGAACCCAAGA |
| | Rv | TTCGGCCGTGATTTTCATTAG |
| | Pr | FAM/AAAAGAAGGCACGAAGAA/MGB |
| ZIKV | Fw | GACATGGCTTCGGACAG |
| | Rv | CTTTGCCAAAAAGTCCACA |
| YFV | Fw | GCTAATTGAGGTGYATTGGTCTGC |
| | Rv | CTGCTAATCGCTCAAMGAACG |
| | Pr | 56-FAM/ATCGAGTTG/ZEN/CTAGGCAATAAACAC/3IABkFQ |
| JEV | Fw | AGCTGGGCCTTCTGGT |
| | Rv | CCCAAGCATCAGCACAAG |
| | Pr | 56-FAM/CTTCGCAAG/ZEN/AGGTGGACGGCCA/3IABkFQ |
| WNV | Fw | AAGTTGAGTAGACGGTGCTG |
| | Rv | AGACGGTTCTGAGGGCTTAC |
| | Pr | 56-FAM/GCTCAACCCAGGAGGACTGG/MGBEQ |
| CHIKV | Fw | AAGCTYCGCGTCTTTACCAAG |
| | Rv | CCAATTGTCCYGGTCTTCT |
| | Pr | 56-FAM/CCAATGTCT/ZEN/TCAGCCTGGACACCTTT/3IABkFQ |
| HCoV-229E | Fw | CAGTCAAATGGGCTGATGCA |
| | Rv | CAAAGGGCTATAAAGAGAATAAGGTATTCT |
| | Pr | 56-FAM/TGAACCACA/ZEN/ACGTGGTCGTCAGGG/3IABkFQ |
| HCoV-OC43 | Fw | CGATGAGGCTATTCCGACTAGGT |
| | Rv | CTTCCTGAGCCTTCAATATAGTAACC |
| | Pr | 56-FAM/TCCGCCTGG/ZEN/CACGGTACTCCCT/3IABkFQ |
| SARS-CoV | Fw | GGAGCCTGAATACACCCAAAG |
| | Rv | GCACGGTGGCAGCATTG |
| | Pr | 56-FAM/CCACATTGG/ZEN/CACCCGCAATCC/3IABkFQ |
| MERS-CoV | Fw | CAAAACCTCCCTAAGAAGGAAAAG |
| | Rv | GCTCCTTTGGAGGTTTCAGACAT |
| | Pr | 56-FAM/ACAAAAGGC/ZEN/ACCAAAAGAAGAATCAACAGACC/3IABkFQ |
| SARS-CoV-2 | Fw | CACATTGGCACCCGCAATC |
| | Rv | GAGGAACGAGAAGAGGCTTG |
| | Pr | 56-FAM/ACTTCCTCA/ZEN/AGGAACAACATTGCCA/3IABkFQ |
| RABV | Fw | GCCACGGTTATTGCTGCAT |
| | Rv | CTCCCAAATAGCCCCCTAGAA |
| | Pr | FAM/CCCTCATGAGATGTC/MGB |
| RVFV | Fw | TTCTTTGCTTCTGATACCCTCTG |
| | Rv | GTTCCACTTCTTGCATCATCTG |
| | Pr | 56-FAM/TTGCACAAG/ZEN/TCCACACAGGCCCT/3IABkFQ |
| HSV-1 | Fw | GGGCCGTGATTTTGTGTC |
| | Rv | CCGCCAAGGCATATTTGC |
| | Pr | FAM/TAGTGGGCCTCCATGGG/MGB |
| ACTB (<i>C.aethiops</i>) | Fw | GCTGCCCTGAGGCTCTT |
| | Rv | TGATGGAGTTGAAGGTAGTTTCATG |

1331 **SI references**

1332

- 1333 1. S. Shresta, K. L. Sharar, D. M. Prigozhin, P. R. Beatty, E. Harris, Murine
1334 Model for Dengue Virus-Induced Lethal Disease with IncreasedVascular
1335 Permeability. *J. Virol.* **80**, 10208–10217 (2006).
- 1336 2. H. Gu, *et al.*, Adaptation of SARS-CoV-2 in BALB/c mice for testing
1337 vaccine efficacy. *Science (80-.)*. **369**, 1603–1607 (2020).
- 1338 3. S. R. Leist, *et al.*, A Mouse-Adapted SARS-CoV-2 Induces Acute Lung
1339 Injury and Mortality in Standard Laboratory Mice. *Cell* **183**, 1070-
1340 1085.e12 (2020).
- 1341 4. X. Chen, A. Murawski, K. Patel, C. L. Crespi, P. V. Balimane, A novel
1342 design of artificial membrane for improving the PAMPA model. *Pharm.*
1343 *Res.* **25**, 1511–1520 (2008).
- 1344 5. P. Shah, *et al.*, An automated high-throughput metabolic stability assay
1345 using an integrated high-resolution accurate mass method and automated
1346 data analysis software. *Drug Metab. Dispos.* **44**, 1653–1661 (2016).

1347